Renormalization of the $0\nu\beta\beta$ operator within the realistic shell model

Luigi Coraggio

Istituto Nazionale di Fisica Nucleare - Sezione di Napoli

July 18th, 2019
ECT*, Trento

Acknowledgements

- A. Gargano (INFN-NA)
- N. Itaco (UNICAMPANIA and INFN-NA)
- R. Mancino (UNICAMPANIA and INFN-NA)
- F. Nowacki (IPHC Strasbourg and UNICAMPANIA)
- L. C. (INFN-NA)

Outline

- The calculation of the nuclear matrix element $M^{0\nu}$ of $0\nu\beta\beta$ decay
- The realistic nuclear shell model (RSM)
- Present work:
  - Testing the RSM: calculation of spectroscopic properties, GT strengths, and the nuclear matrix elements of $2\nu\beta\beta$ decay
  - RSM calculation of $0\nu\beta\beta$ nuclear matrix element $M^{0\nu}$ and comparison with other SM results
  - Perturbative properties of the $0\nu\beta\beta$ effective operator
  - Evaluation of the $M^{0\nu}$
- Outlook

Candidates to the detection of the $0\nu\beta\beta$-decay

- The main factors to locate the nuclei that are the best candidates to detect the $0\nu\beta\beta$-decay are:
  - the Q-value;
  - the phase-space factor $G^{0\nu}$;
  - the isotopic abundance

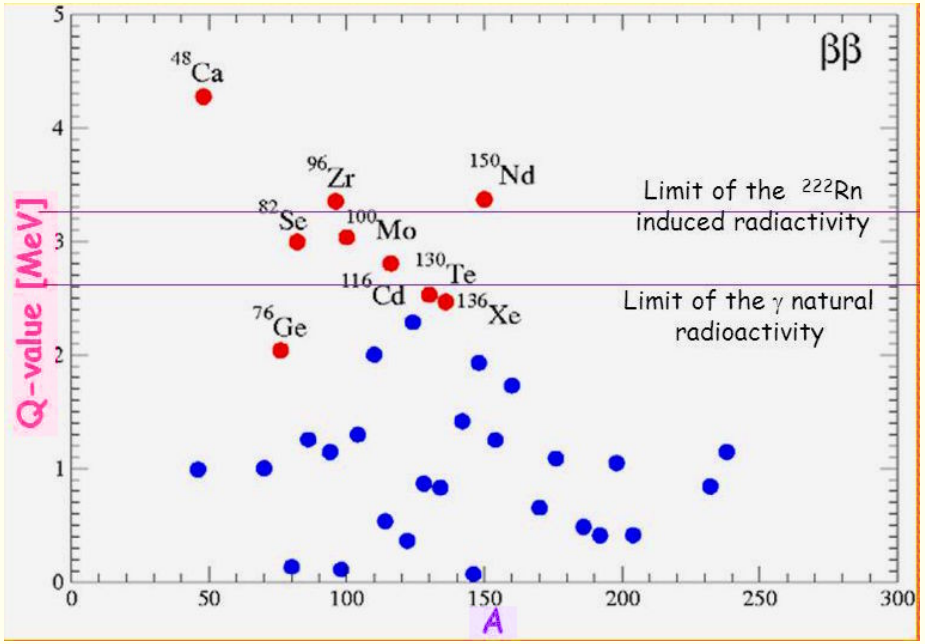

- First group: ^{76}Ge, ^{130}Te, and ^{136}Xe.
- Second group: ^{82}Se, ^{100}Mo, and ^{116}Cd.
- Third group: ^{48}Ca, ^{96}Zr, and ^{150}Nd.

The calculation of $M^{0\nu}$

To describe the nuclear properties detected in the experiments, one needs to resort to nuclear structure models.

- Every model is characterized by a certain number of parameters.
- The calculated value of $M^{0\nu}$ may depend upon the chosen nuclear structure model.

All models may present advantages and/or shortcomings to calculate $M^{0\nu}$

Nuclear structure calculations

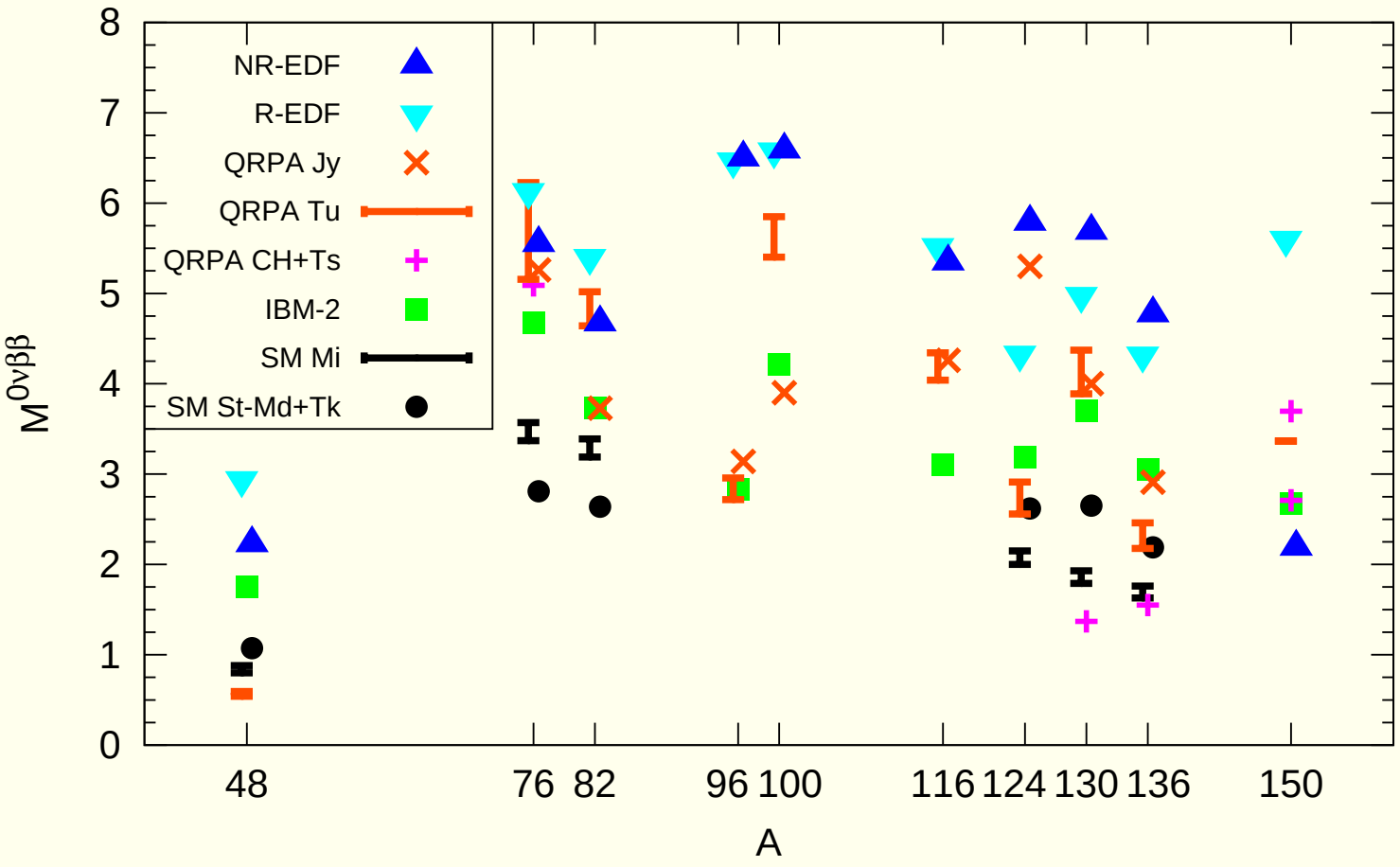

- The spread of nuclear structure calculations evidences inconsistencies among results obtained with different models

The renormalization of g_A, g_V

There are some arguments to employ $g_A^{\rm eff}, g_V^{\rm eff}$.
Effective coupling constants are necessary to take into account:

- the degrees of freedom that have been excluded because of the truncation of the Hilbert space;
- the short-range correlations excluded to soften the NN force, when starting from realistic potentials;
- contributions to the free values of g_A, g_V from meson exchange currents.

In this study we tackle the first two issues deriving effective-decay operators by way of the many-body perturbation theory

- *H. Q. Song, H. F. Wu, T. T. S. Kuo, Phys. Rev. C* **40**, *2260 (1989)*
- *A. Staudt, T. T. S. Kuo, H. V. Klapdor-Kleingrothaus, Phys. Rev. C* **46**, *871 (1992)*
- *J. D. Holt and J. Engel, Phys. Rev. C* **87**, *064315 (2013)*

Effective shell-model hamiltonian

The shell-model hamiltonian has to take into account all the degrees of freedom not explicitly considered in an effective way

Two alternative approaches

- phenomenological
- microscopic

$$V_{NN} \ (+V_{NNN}) \Rightarrow \text{many-body theory} \Rightarrow H_{\text{eff}}$$

Definition

The eigenvalues of H_{eff} belong to the set of eigenvalues of the full nuclear hamiltonian.
This may be provided by a similarity transformation Ω of the full Hilbert-space hamiltonian H

An example: ^{19}F

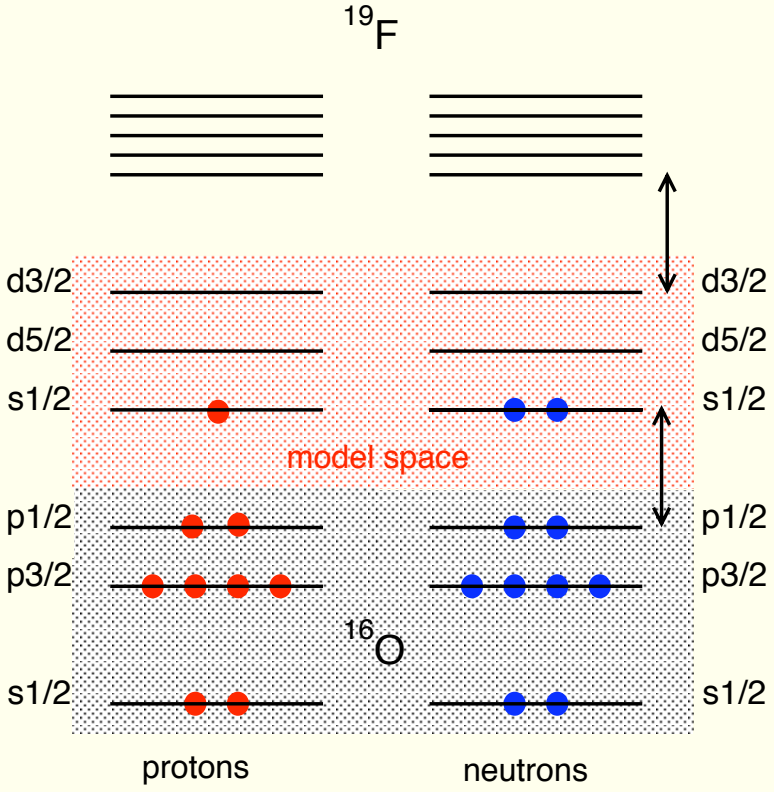

- 9 protons & 10 neutrons interacting in the full Hilbert space
- spherically symmetric mean field (e.g. harmonic oscillator)
- 1 valence proton & 2 valence neutrons interacting in a truncated model space

The degrees of freedom of the core nucleons and the excitations of the valence ones above the model space are not considered explicitly.

Workflow for a realistic shell-model calculation

1. Choose a realistic *NN* potential (*NNN*)
2. Renormalize its short range correlations
3. Identify the model space better tailored to study the physics problem
4. Derive the effective shell-model hamiltonian and consistently effective transition operators, by way of the many-body perturbation theory
5. Calculate the observables (energies, e.m. transition probabilities, β-decay amplitudes...), using only theoretical SP energies, two-body matrix elements, and effective operators.

INFN
Istituto Nazionale di Fisica Nucleare

Realistic nucleon-nucleon potential: V_{NN}

Several realistic potentials $\chi^2/datum \simeq 1$:
CD-Bonn, Argonne V18, Nijmegen, ...

Strong short-range repulsion

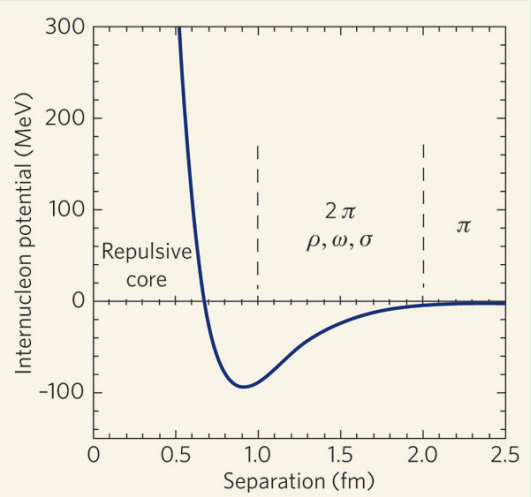

How to handle the short-range repulsion ?

- Brueckner G matrix
- EFT inspired approaches
  - $V_{\mathrm{low-k}}$, our chosen cutoff: $\Lambda = 2.6$ fm^{-1}
  - SRG

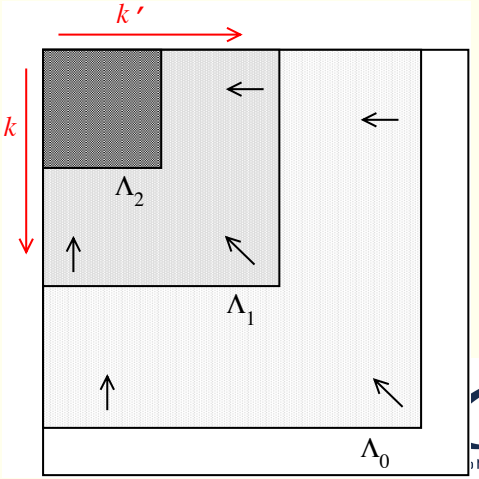

The shell-model effective hamiltonian

We start from the many-body hamiltonian H defined in the full Hilbert space:

$$H = H_0 + H_1 = \sum_{i=1}^{A}(T_i + U_i) + \sum_{i<j}(V_{ij}^{NN} - U_i)$$

$$\left(\begin{array}{c|c} PHP & PHQ \\ \hline QHP & QHQ \end{array}\right) \quad \begin{array}{c} \mathcal{H} = \Omega^{-1} H \Omega \\ \Longrightarrow \\ Q\mathcal{H}P = 0 \end{array} \quad \left(\begin{array}{c|c} P\mathcal{H}P & P\mathcal{H}Q \\ \hline 0 & Q\mathcal{H}Q \end{array}\right)$$

$$H_{\text{eff}} = P\mathcal{H}P$$

Suzuki & Lee $\Rightarrow \Omega = e^{\omega}$ with $\omega = \left(\begin{array}{c|c} 0 & 0 \\ \hline Q\omega P & 0 \end{array}\right)$

$$H_1^{\text{eff}}(\omega) = PH_1P + PH_1Q\frac{1}{\epsilon - QHQ}QH_1P - \\ -PH_1Q\frac{1}{\epsilon - QHQ}\omega H_1^{\text{eff}}(\omega)$$

The perturbative approach to the shell-model H^{eff}

The $\hat{Q}$-box vertex function

$$\hat{Q}(\epsilon) = PH_1P + PH_1Q\frac{1}{\epsilon - QHQ}QH_1P$$

Exact calculation of the $\hat{Q}$-box is computationally prohibitive for many-body system $\Rightarrow$ we perform a perturbative expansion

$$\frac{1}{\epsilon - QHQ} = \sum_{n=0}^{\infty}\frac{(QH_1Q)^n}{(\epsilon - QH_0Q)^{n+1}}$$

$\hat{Q}$-box: 1st- & 2nd-order 1-b diagrams

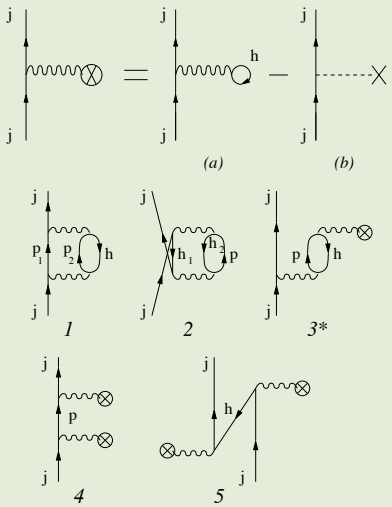

$\hat{Q}$-box: 1st- & 2nd-order 2-b diagrams

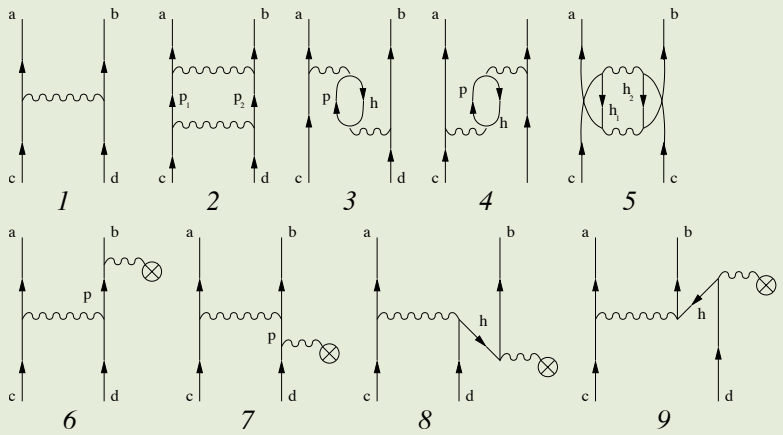

$\hat{Q}$-box perturbative expansion

$\hat{Q}$-box: 3rd-order 1-b diagrams

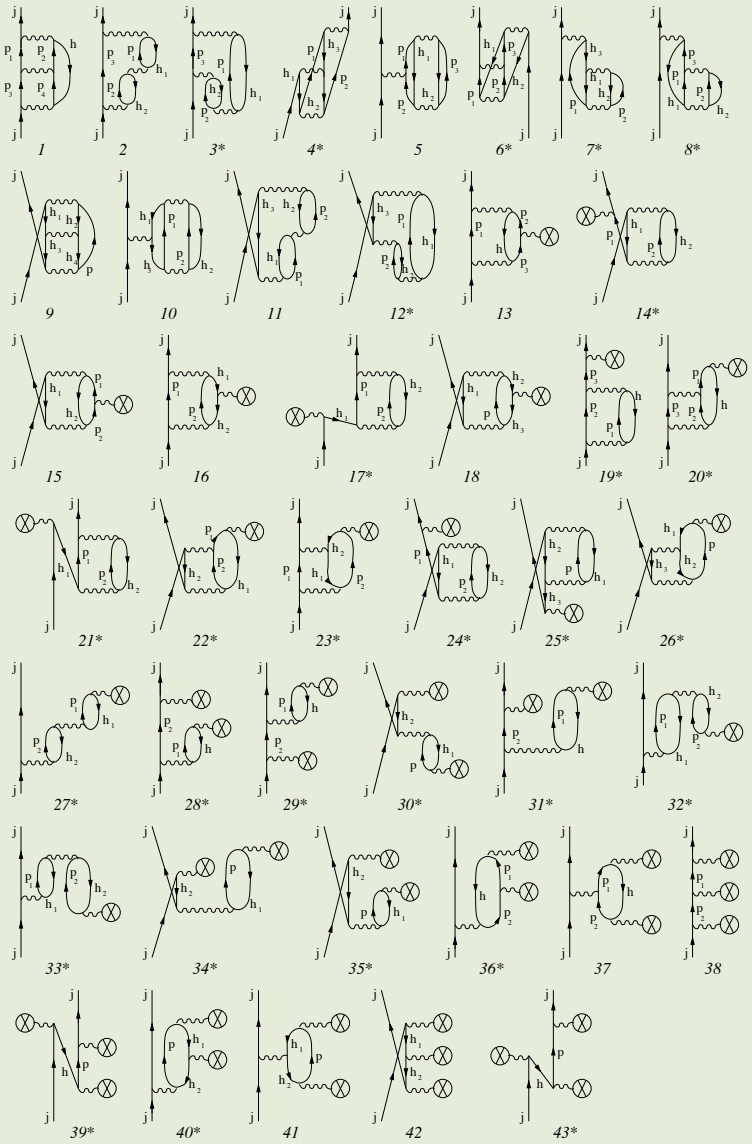

$\hat{Q}$-box: 3rd-order 2-b diagrams

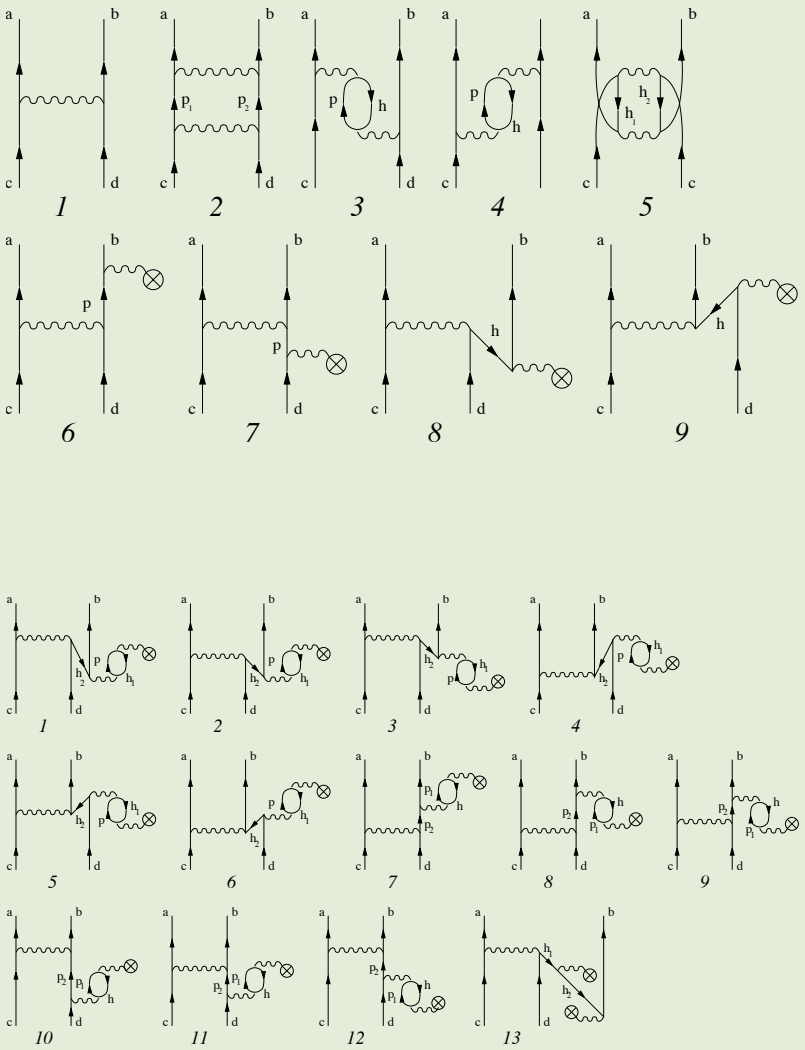

$\hat{Q}$-box perturbative expansion

$\hat{Q}$-box: 3rd-order 2-b diagrams

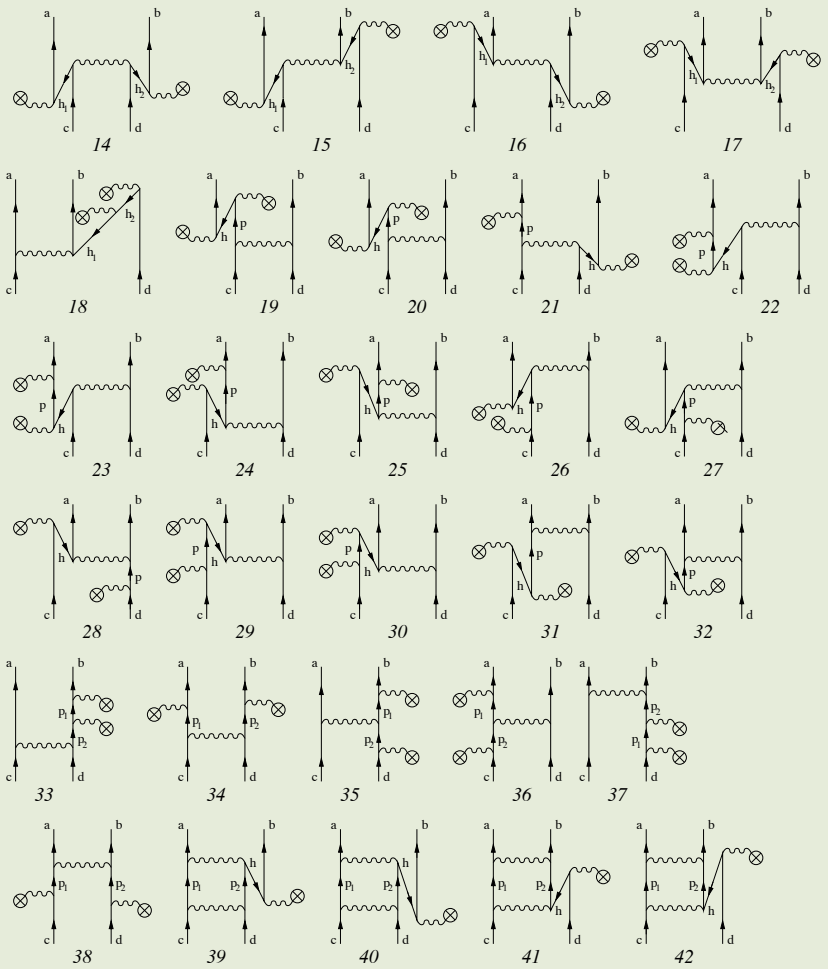

$\hat{Q}$-box: 3rd-order 2-b diagrams

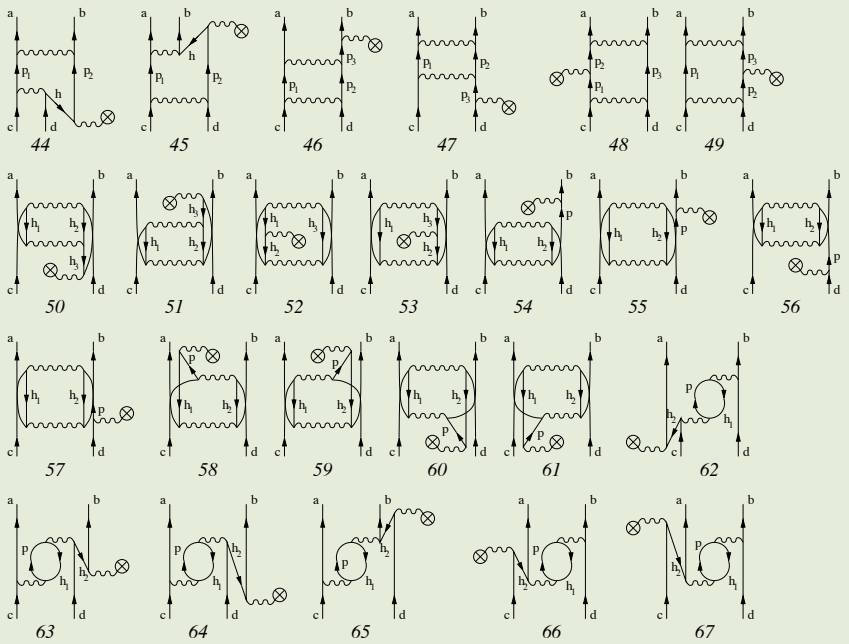

L.C., A. Covello, A. Gargano, N. Itaco, and T. T. S. Kuo, Ann. Phys. **327** *, 2125-2151 (2012)*

$\hat{Q}$-box perturbative expansion

$\hat{Q}$-box: 3rd-order 2-b diagrams

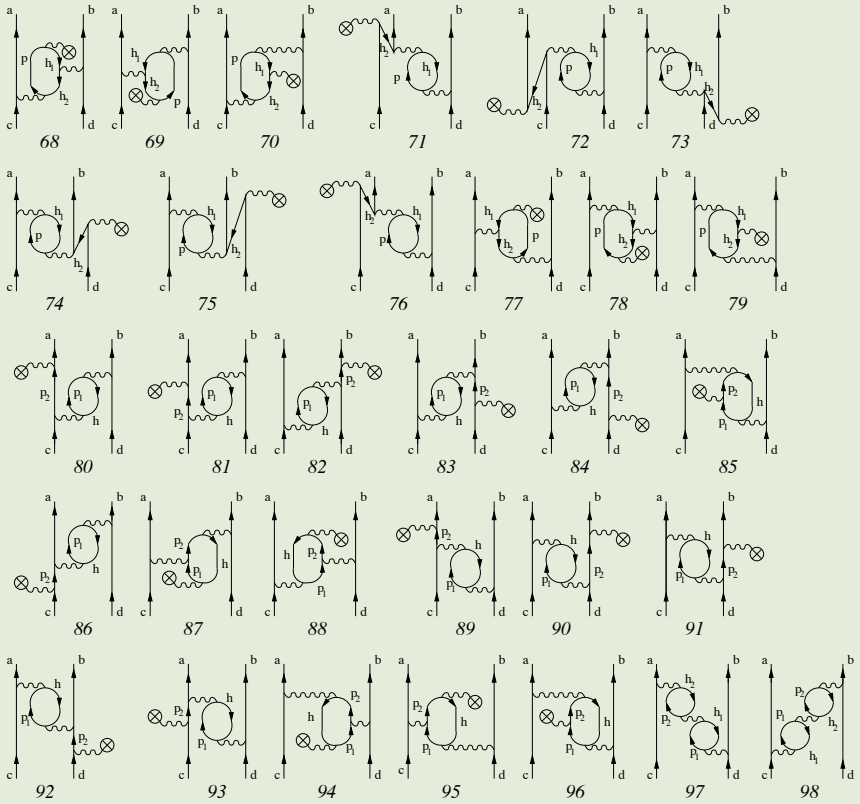

L.C., A. Covello, A. Gargano, N. Itaco, and T. T. S. Kuo, Ann. Phys. **327** *, 2125-2151 (2012)*

$\hat{Q}$-box: 3rd-order 2-b diagrams

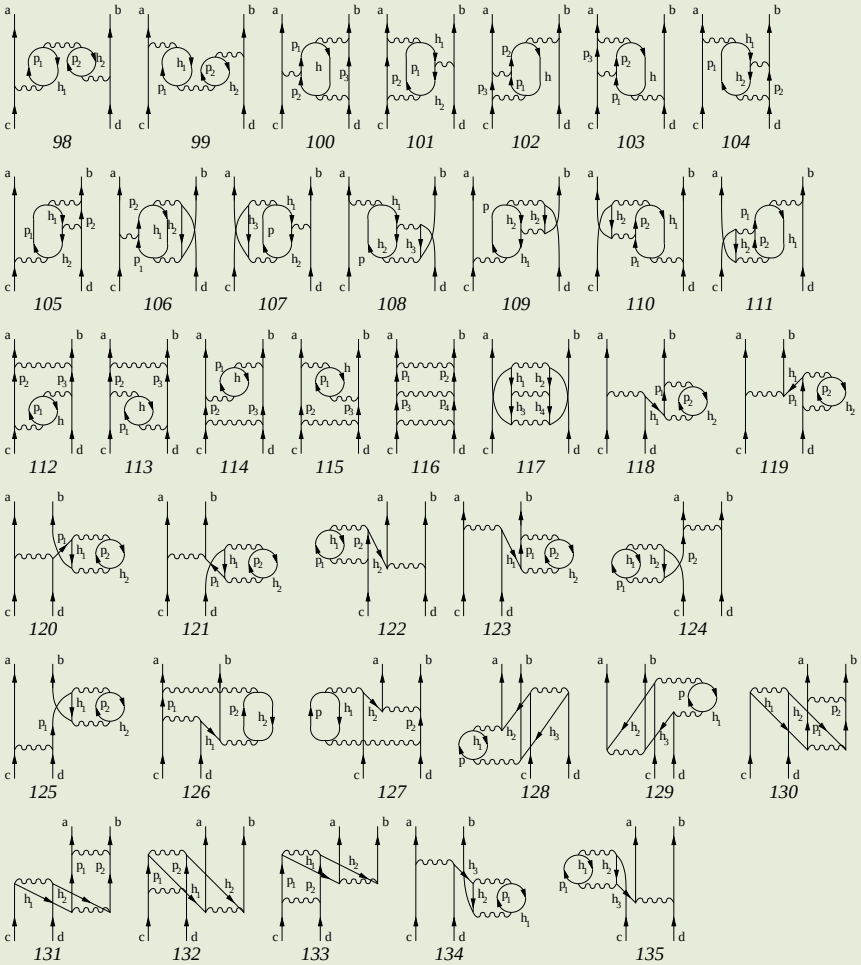

Effective operators for decay amplitudes

- Ψ_α indicates eigenstates of the full hamiltonian H corresponding to eigenvalues E_α
- Φ_α indicates the eigenvectors obtained diagonalizing H_{eff} in the reduced model space P and corresponding to the same eigenvalues E_α

$$\Rightarrow |\Phi_\alpha\rangle = P\,|\Psi_\alpha\rangle$$

Obviously, for any decay-operator Θ:

$$\langle\Phi_\alpha|\Theta|\Phi_\beta\rangle \neq \langle\Psi_\alpha|\Theta|\Psi_\beta\rangle$$

We then require an effective operator Θ_{eff} defined as follows

$$\Theta_{\text{eff}} = \sum_{\alpha\beta} |\Phi_\alpha\rangle\,\langle\Psi_\alpha|\Theta|\Psi_\beta\rangle\,\langle\Phi_\beta|$$

Consequently, the matrix elements of Θ_{eff} are

$$\langle\Phi_\alpha|\Theta_{\text{eff}}|\Phi_\beta\rangle = \langle\Psi_\alpha|\Theta|\Psi_\beta\rangle$$

The shell-model effective operators

Any shell-model effective operator may be derived consistently with the $\hat{Q}$-box-plus-folded-diagram approach to $H_{\rm eff}$

It has been demonstrated that, for any bare operator Θ, a non-Hermitian effective operator $\Theta_{\rm eff}$ can be written in the following form:

$$\Theta_{\rm eff} = (P + \hat{Q}_1 + \hat{Q}_1\hat{Q}_1 + \hat{Q}_2\hat{Q} + \hat{Q}\hat{Q}_2 + \cdots)(\chi_0 + \\ + \chi_1 + \chi_2 + \cdots) \ ,$$

where

$$\hat{Q}_m = \frac{1}{m!}\frac{d^m\hat{Q}(\epsilon)}{d\epsilon^m}\bigg|_{\epsilon=\epsilon_0} \ ,$$

ϵ_0 being the model-space eigenvalue of the unperturbed hamiltonian H_0

K. Suzuki and R. Okamoto, Prog. Theor. Phys. **93** *, 905 (1995)*

The shell-model effective operators

The χ_n operators are defined as follows:

$$
\begin{aligned}
\chi_0 &= (\hat{\Theta}_0 + h.c.) + \Theta_{00} \ , \\
\chi_1 &= (\hat{\Theta}_1 \hat{Q} + h.c.) + (\hat{\Theta}_{01} \hat{Q} + h.c.) \ , \\
\chi_2 &= (\hat{\Theta}_1 \hat{Q}_1 \hat{Q} + h.c.) + (\hat{\Theta}_2 \hat{Q}\hat{Q} + h.c.) + \\
&\quad (\hat{\Theta}_{02} \hat{Q}\hat{Q} + h.c.) + \hat{Q}\hat{\Theta}_{11}\hat{Q} \ , \\
&\quad \ldots
\end{aligned}
$$

and

$$
\hat{\Theta}(\epsilon) = P\Theta P + P\Theta Q \frac{1}{\epsilon - QHQ} QH_1 P
$$

$$
\hat{\Theta}(\epsilon_1;\epsilon_2) = PH_1 Q \frac{1}{\epsilon_1 - QHQ} \times Q\Theta Q \frac{1}{\epsilon_2 - QHQ} QH_1 P
$$

$$
\hat{\Theta}_m = \frac{1}{m!} \frac{d^m \hat{\Theta}(\epsilon)}{d\epsilon^m}\bigg|_{\epsilon=\epsilon_0}
$$

$$
\hat{\Theta}_{nm} = \frac{1}{n!m!} \frac{d^n}{d\epsilon_1^n} \frac{d^m}{d\epsilon_2^m} \hat{\Theta}(\epsilon_1;\epsilon_2)\bigg|_{\epsilon_{1,2}=\epsilon_0}
$$

Istituto Nazionale di Fisica Nucleare

The shell-model effective operators

We arrest the χ series at χ_2 term, and then expand $\hat{\Theta}$ perturbatively:

One-body operator

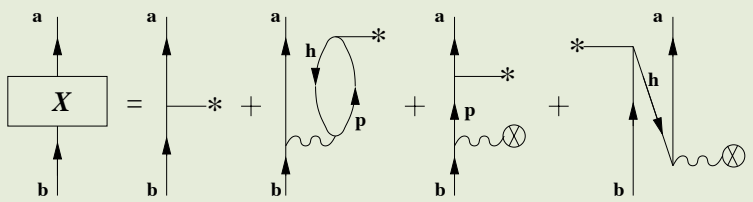

Two-body operator

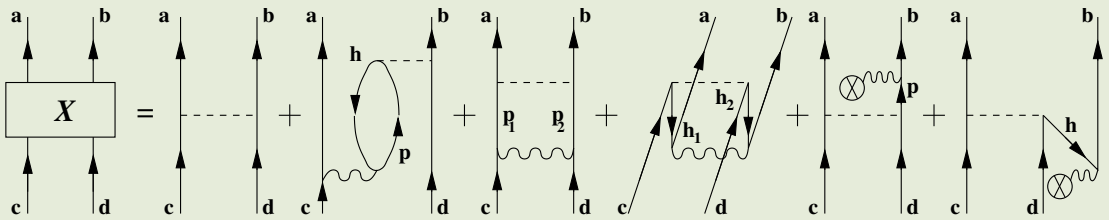

- *E. M. Krenciglowa and T. T. S. Kuo, Nucl. Phys. A* **240**, *195 (1975)*
- *I. S. Towner, Phys. Rep.* **155**, *263 (1987)*
- *H. Q. Song, H. F. Wu, T. T. S. Kuo, Phys. Rev. C* **40**, *2260 (1989)*
- *J. D. Holt and J. Engel, Phys. Rev. C* **87**, *064315 (2013).*
- *L.C., L. De Angelis, T. Fukui, A. Gargano, and N. Itaco, Phys. Rev. C* **95**, *064324 (2017).*

The choice of the cutoff $\Lambda = 2.6\ \mathrm{fm}^{-1}$

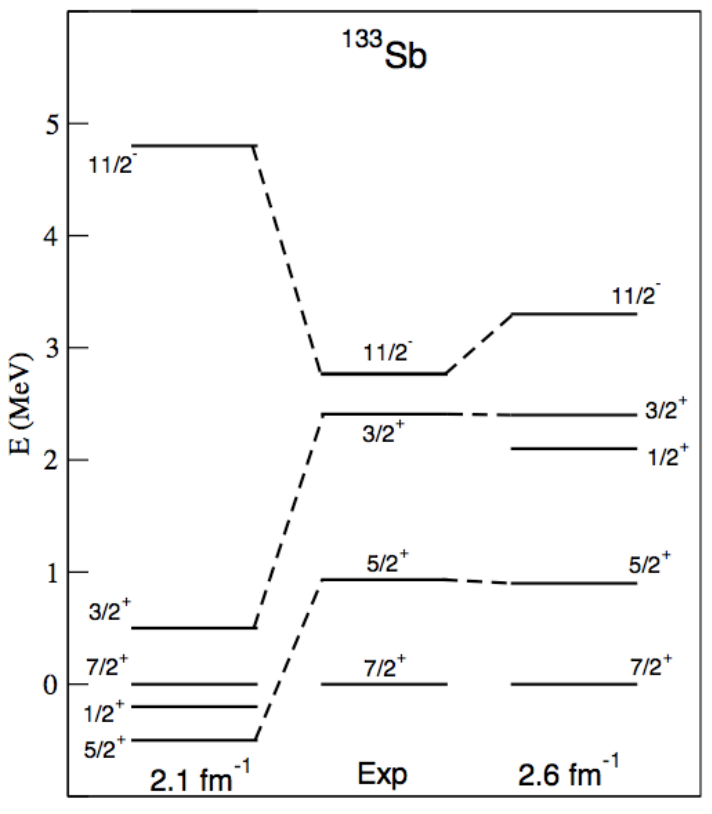

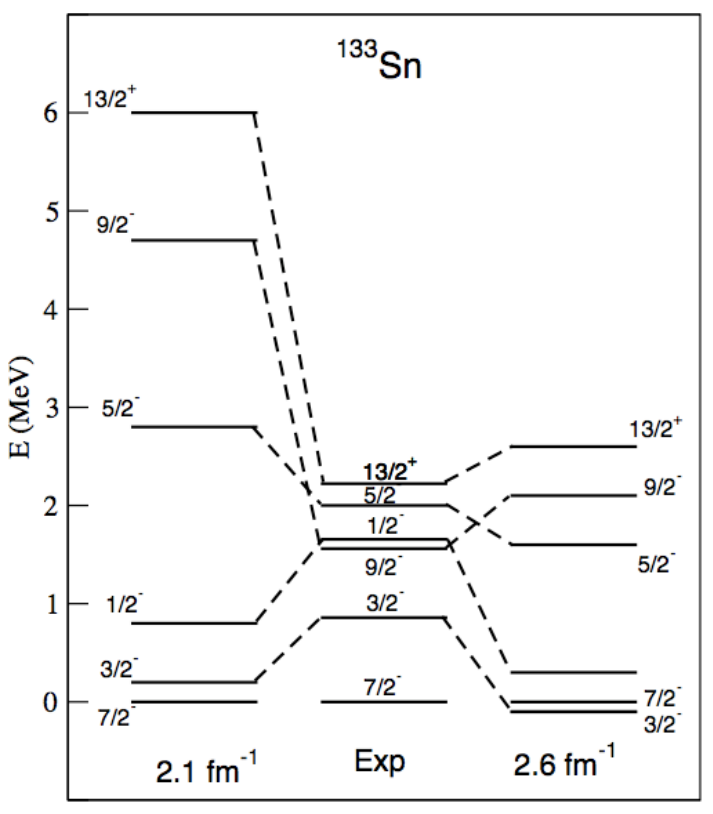

Choosing a larger cutoff ("hard potential") corresponds to reduce the role of three-body forces

L. C., A. Gargano, and N. Itaco, JPS Conf. Proc. **6**, *020046 (2015)*

Nuclear models and predictive power

Nuclear model → Accurate reproduction of experimental data

↓

Predictive power

Realistic SM calculations of spectroscopic properties for ^{48}Ca, ^{76}Ge, ^{82}Se, ^{130}Te, and ^{136}Xe

$\Downarrow$

Check our approach calculating GT strengths and $2\nu\beta\beta$-decay

$$\left[T^{2\nu}_{1/2}\right]^{-1} = G^{2\nu}\left|M^{2\nu}_{\mathrm{GT}}\right|^2$$

where

$$M^{\mathrm{GT}}_{2\nu} = \sum_n \frac{\langle 0^+_f||\vec{\sigma}\tau^-||1^+_n\rangle\langle 1^+_n||\vec{\sigma}\tau^-||0^+_i\rangle}{E_n + E_0}$$

Model spaces

- ^{48}Ca: four proton and neutron orbitals outside doubly-closed ^{40}Ca
  $0f_{7/2}, 0f_{5/2}, 1p_{3/2}, 1p_{1/2}$
- ^{76}Ge,^{82}Se: four proton and neutron orbitals outside doubly-closed ^{56}Ni
  $0f_{5/2}, 1p_{3/2}, 1p_{1/2}, 0g_{9/2}$
- ^{130}Te,^{136}Xe: five proton and neutron orbitals outside doubly-closed ^{100}Sn
  $0g_{7/2}, 1d_{5/2}, 1d_{3/2}, 2s_{1/2}, 0h_{11/2}$

Spectroscopic properties

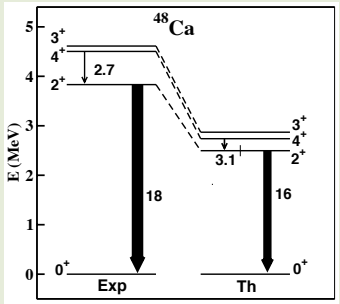

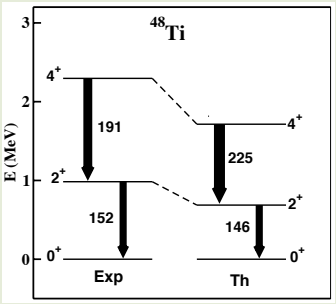

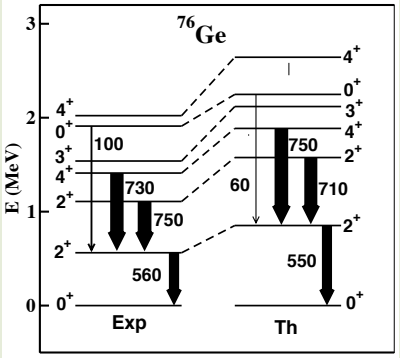

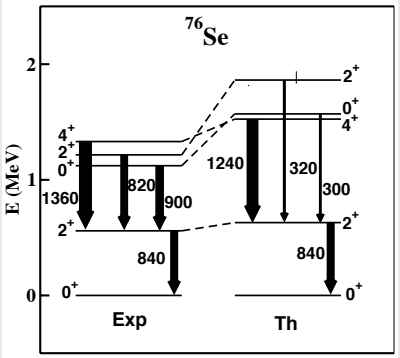

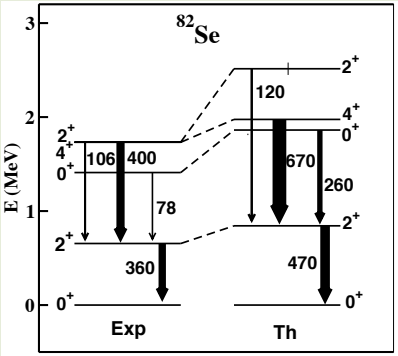

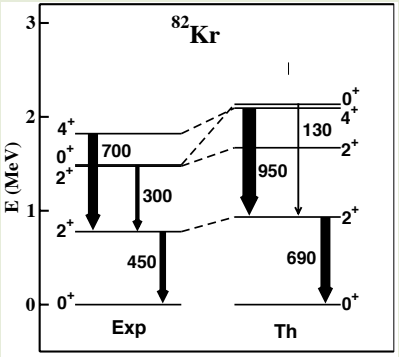

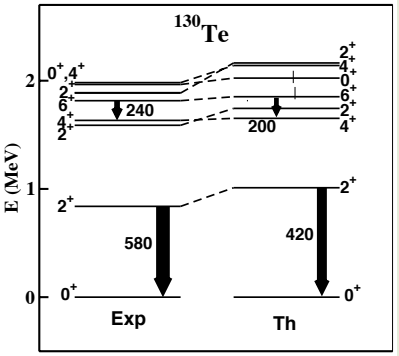

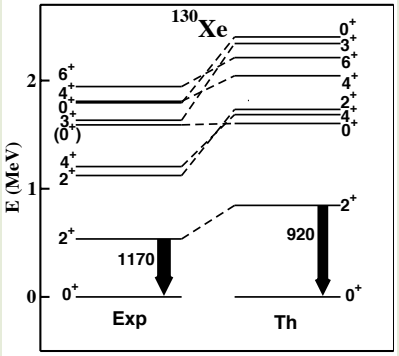

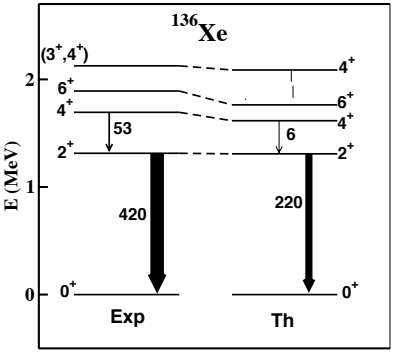

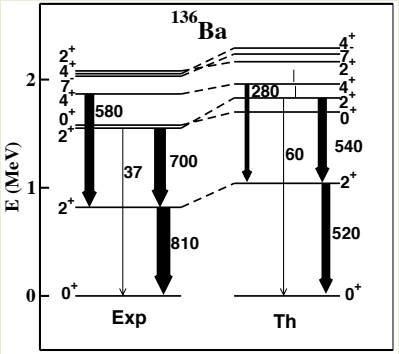

Properties of effective spin-dependent $M1$ operator

Nucleus	$J_i \to J_f$	$B(M1)_{\mathrm{Expt}}$	bare	effective
^{48}Ca				
	$3_1^+ \to 2_1^+$	0.023 ± 0.004	0.051	0.046
^{76}Ge				
	$2_2^+ \to 2_1^+$	$0.003^{+0.002}_{-0.003}$	0.006	0.005
	$4_2^+ \to 3_1^+$	0.02 ± 0.01	0.06	0.03
	$4_2^+ \to 4_1^+$	$0.03^{+0.02}_{-0.03}$	0.07	0.03
^{130}Te				
	$2_3^+ \to 2_1^+$	$0.097^{+0.08}_{-0.11}$	0.057	0.077

Nucleus	J	μ_{Expt}	bare	effective
^{48}Ti				
	2_1^+	$+0.78 \pm 0.04$	+0.37	+0.54
	4_1^+	$+2.2 \pm 0.5$	+1.2	+1.5
^{76}Ge				
	2_1^+	$+0.64 \pm 0.02$	+0.53	+0.84
	2_2^+	$+0.78 \pm 0.10$	+0.93	+1.09
	4_1^+	$+0.96 \pm 0.68$	+0.58	+1.36
^{76}Se				
	2_1^+	0.81 ± 0.05	+0.37	+0.58
	2_2^+	0.70 ± 0.12	+0.64	+0.79
	4_1^+	2.6 ± 0.4	+0.3	+0.9

Properties of effective spin-dependent $M1$ operator

Nucleus	$J_i \to J_f$	$B(M1)_{\mathrm{Expt}}$	bare	effective
^{136}Ba				
	$2_2^+ \to 2_1^+$	0.02 ± 0.1	0.07	0.06
	$2_3^+ \to 2_1^+$	0.002 ± 0.002	0.006	0.001
	$4_2^+ \to 4_1^+$	$0.06^{+0.08}_{-0.05}$	0.15	0.09

Nucleus	J	μ_{Expt}	bare	effective
^{82}Se				
	2_1^+	$+0.99 \pm 0.06$	+0.72	+1.05
	4_1^+	2.3 ± 1.5	+1.2	+1.9
^{82}Kr				
	2_1^+	$+0.80 \pm 0.04$	+0.50	+0.83
	4_1^+	$+1.2 \pm 0.8$	+0.5	+1.3
^{130}Te				
	2_1^+	0.58 ± 0.10	+0.52	+0.71
^{130}Xe				
	2_1^+	0.57 ± 0.14	+0.50	+0.66
^{136}Xe				
	2_1^+	1.53 ± 0.09	+1.05	+1.14
	4_1^+	3.2 ± 0.6	+2.02	+2.22
^{136}Ba				
	2_1^+	0.69 ± 0.10	+0.48	+0.59

Perturbative properties of the GT effective operator

Convergence with respect the number of intermediate states

Selection rules of the GT operator make the convergence of the effective one with respect to $N_{\max}$ very fast.

The third decimal digit value of $M^{2\nu}_{\mathrm{GT}}$, calculated with effective operator at third order, does not change from $N_{\max} = 12$ on.

Order-by-order convergence

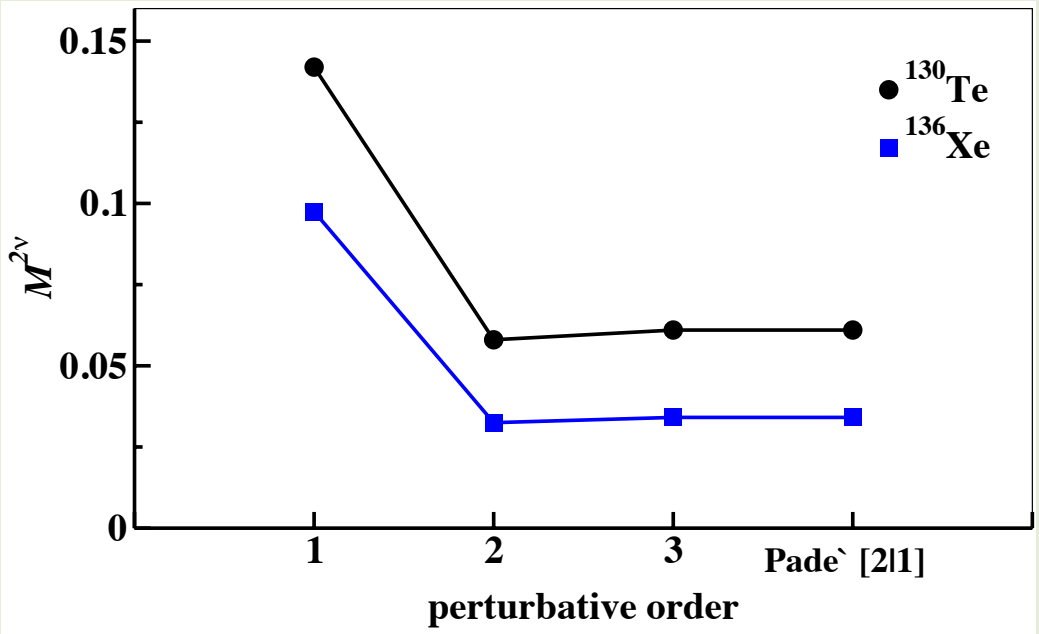

The blocking effect

Blocking (Pauli) effect: the filling of the model-space orbitals by the valence nucleons affects the calculation of the effective GT operator:

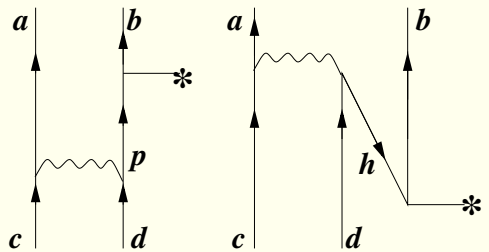

Many-body correlations need to be taken into account: we calculate two-body correlations diagram and sum over one of the incoming/outcoming nucleons

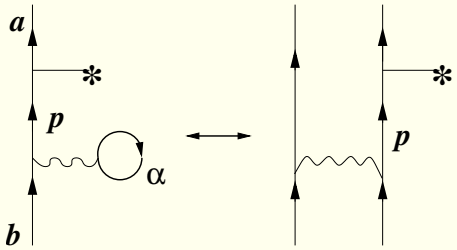

We then obtain a density-dependent one-body GT effective operator
The calculated $M^{2\nu}_{\mathrm{GT}}$ are affected less than 5%

GT⁻ running sums

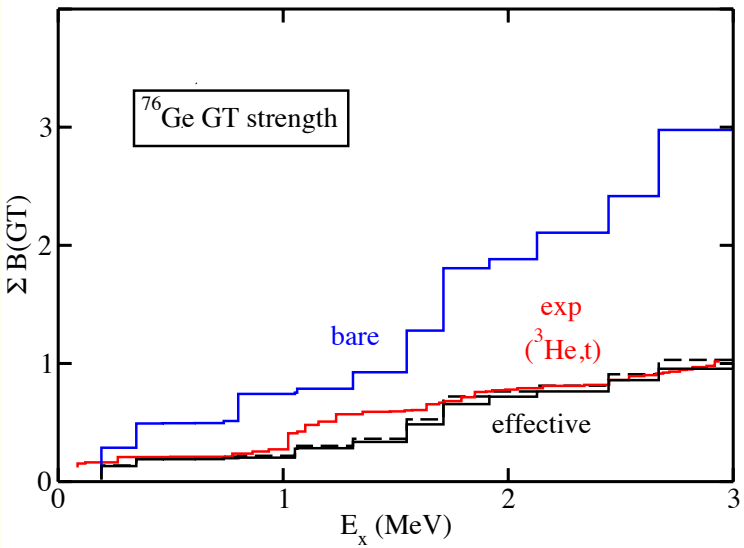

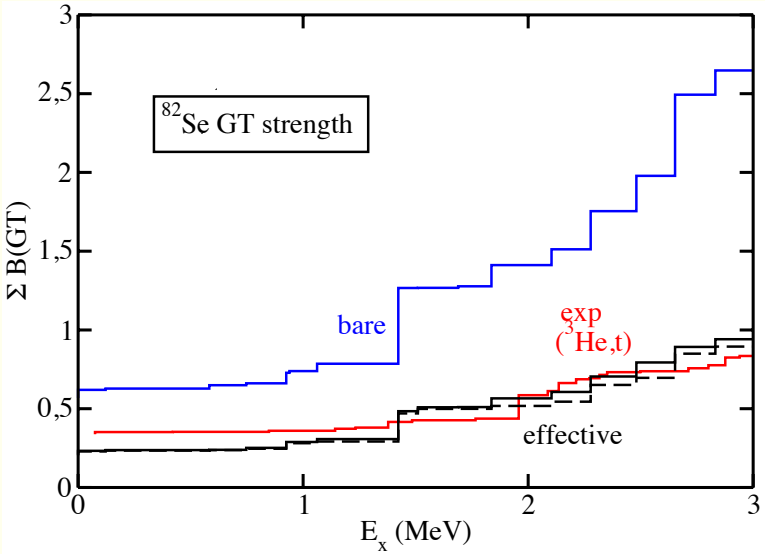

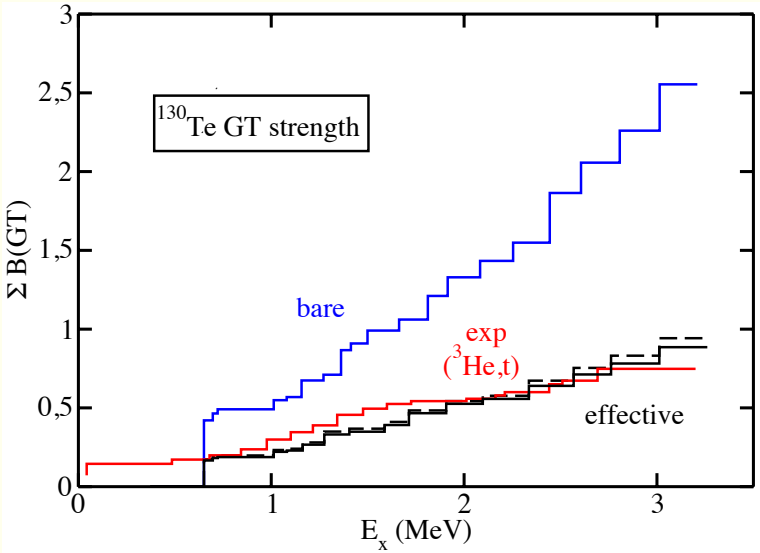

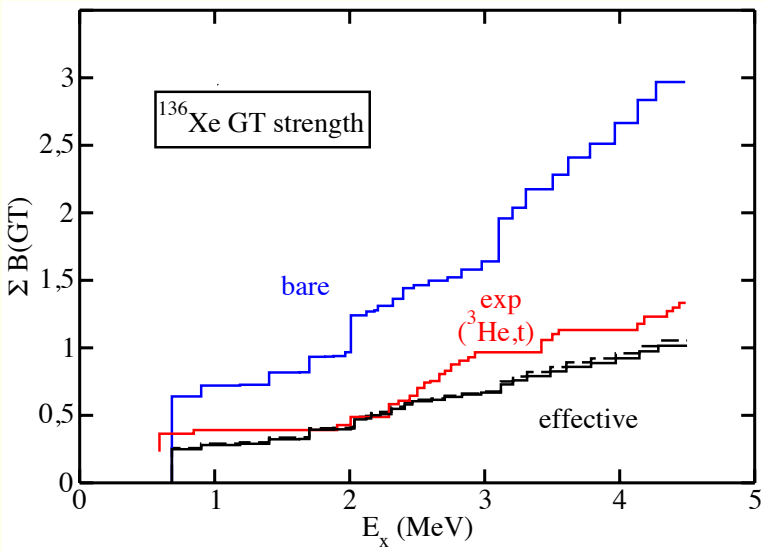

Dashed lines: calculations accounting for the blocking effect

$2\nu\beta\beta$ nuclear matrix elements

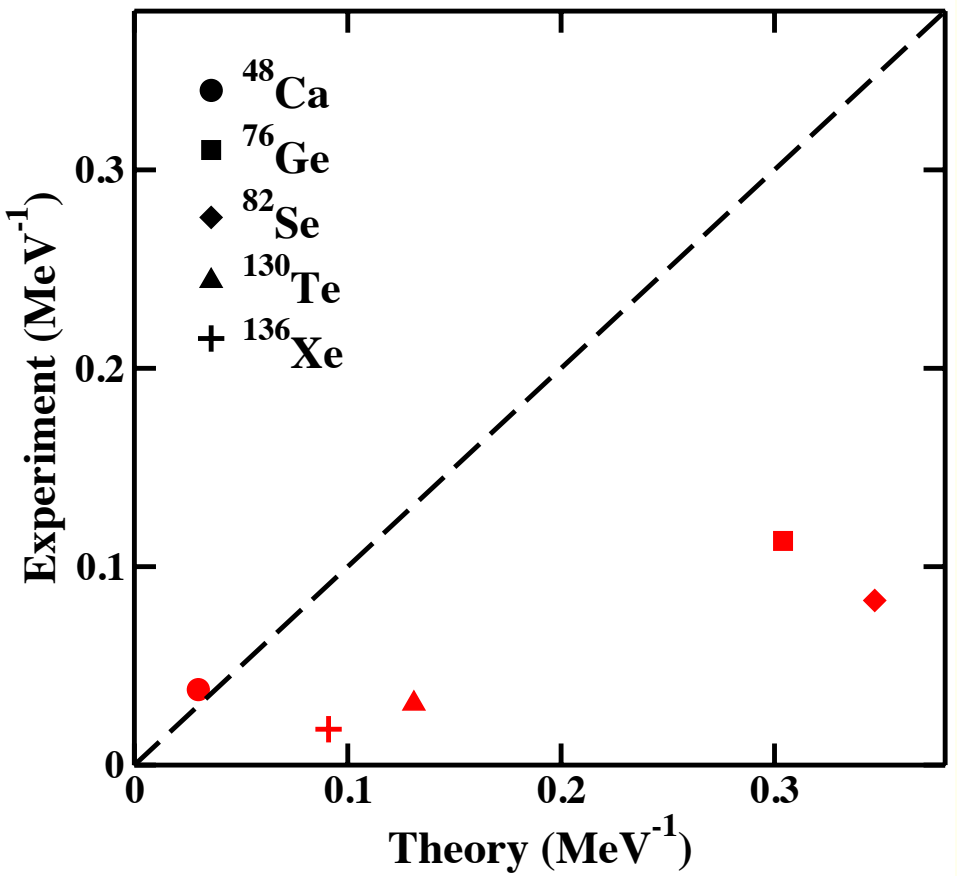

Red dots: bare GT operator

Decay	Expt.	Bare
^{48}Ca $\rightarrow$ ^{48} Ti	0.038 ± 0.003	0.030
^{76}Ge $\rightarrow$ ^{76} Se	0.113 ± 0.006	0.304
^{82}Se $\rightarrow$ ^{82} Kr	0.083 ± 0.004	0.347
^{130}Te $\rightarrow$ ^{130} Xe	0.031 ± 0.004	0.131
^{136}Xe $\rightarrow$ ^{136} Ba	0.0181 ± 0.0007	0.0910

Experimental data from *A. S. Barabash, Nucl. Phys. A* **935**, *52 (2015)*

$2\nu\beta\beta$ nuclear matrix elements

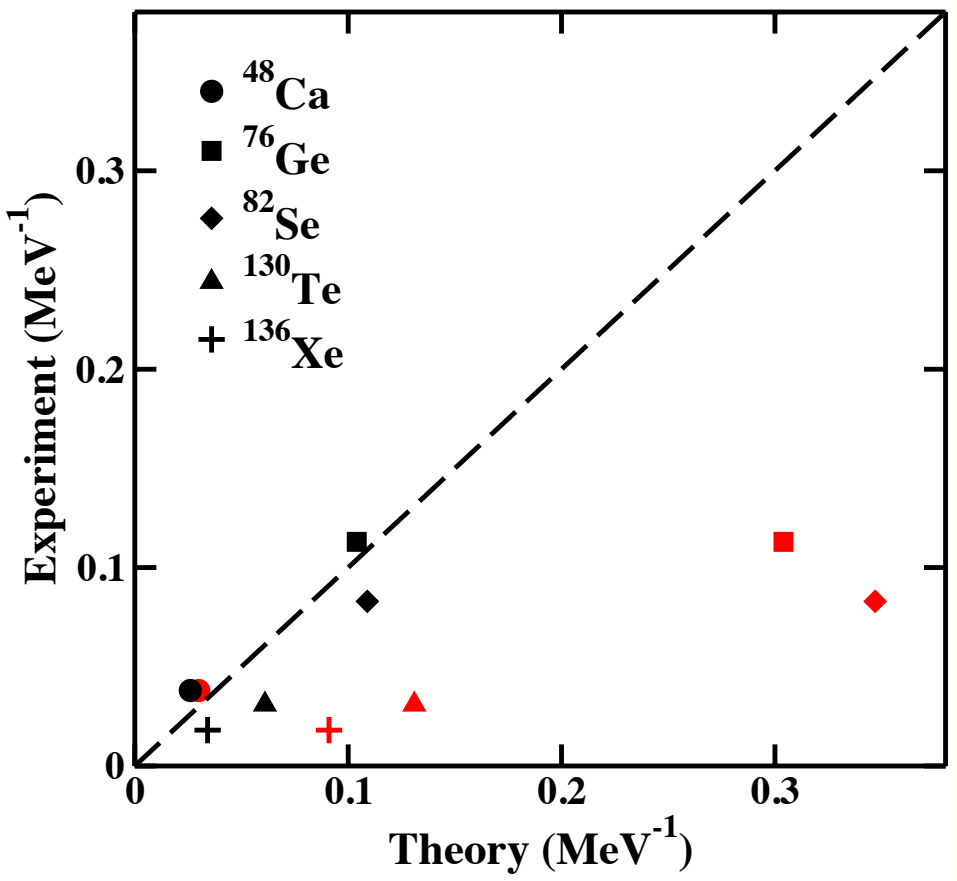

Red dots: bare GT operator
Black triangles: effective GT operator

Decay	Expt.	Eff.
^{48}Ca $\rightarrow$ ^{48} Ti	0.038 ± 0.003	0.026
^{76}Ge $\rightarrow$ ^{76} Se	0.113 ± 0.006	0.104
^{82}Se $\rightarrow$ ^{82} Kr	0.083 ± 0.004	0.109
^{130}Te $\rightarrow$ ^{130} Xe	0.031 ± 0.004	0.061
^{136}Xe $\rightarrow$ ^{136} Ba	0.0181 ± 0.0007	0.0341

Experimental data from *A. S. Barabash, Nucl. Phys. A* **935**, *52 (2015)*

- *L.C., L. De Angelis, T. Fukui, A. Gargano, and N. Itaco, Phys. Rev. C* **95**, *064324 (2017).*
- *L.C., L. De Angelis, T. Fukui, A. Gargano, and N. Itaco (2019), arXiv:1812.04292v2[nucl-th], in press in Phys. Rev. C.*

The calculation of $M^{0\nu}$

The matrix elements $M^{0\nu}_{\alpha}$ are defined as follows:

$$M^{0\nu}_{\alpha} = \sum_{k} \sum_{j_p j_{p'} j_n j_{n'} J_\pi} \langle f | a^\dagger_p a_n | k \rangle \langle k | a^\dagger_{p'} a_{n'} | i \rangle \left\langle j_n j_{n'} ; J^\pi \mid \tau_1^- \tau_2^- O^\alpha_{12} \mid j_p j_{p'} ; J^\pi \right\rangle$$

with $\alpha = (GT,\ F,\ T)$

$$\begin{aligned} O^{GT}_{12} &= \vec{\sigma}_1 \cdot \vec{\sigma}_2 H_{GT}(r) \\ O^{F}_{12} &= H_F(r) \\ O^{T}_{12} &= [3\,(\vec{\sigma}_1 \cdot \hat{r})\,(\vec{\sigma}_1 \cdot \hat{r}) \\ &\quad - \vec{\sigma}_1 \cdot \vec{\sigma}_2]\, H_T(r) \end{aligned}$$

H_α depends on the energy of the initial, final, and intermediate states:

$$H_\alpha(r) = \frac{2R}{\pi} \int_0^\infty \frac{j_\alpha(qr) h_\alpha(q^2) q dq}{q + E_k - (E_i + E_f)/2}$$

Actually, because of the computational complexity, the energies of the intermediate states are replaced by an average value:

$$E_k - (E_i + E_f)/2 \rightarrow \langle E \rangle$$

$$\sum_k \langle f | a^\dagger_p a_n | k \rangle \langle k | a^\dagger_{p'} a_{n'} | i \rangle = \langle f | a^\dagger_p a_n a^\dagger_{p'} a_{n'} | i \rangle$$

The closure approximation

Consequently, the expression of the neutrino potentials becomes:

$$H_\alpha(r) = \frac{2R}{\pi} \int_0^\infty \frac{j_\alpha(qr) h_\alpha(q^2) q dq}{q + < E >}$$

The matrix elements $M_\alpha^{0\nu}$ are then defined, within the closure approximation, as follows:

$$M_\alpha^{0\nu} = \sum_{j_n j_{n'} j_p j_{p'} J_\pi} TBTD\left(j_n j_{n'}, j_p j_{p'}; J_i J_f\right) \left\langle j_n j_{n'}; J^\pi \mid \tau_1^- \tau_2^- O_{12}^\alpha \mid j_p j_{p'}; J^\pi \right\rangle$$

The $TBTD$ are the two-body transition-density matrix elements, and the Gamow-Teller (GT), Fermi (F), and tensor (T) operators:

The closure approximation works since $q \approx$ 100-200 MeV, while model-space excitation energies $E_{exc} \approx$ 10 MeV

Sen'kov and Horoi (Phys. Rev. C **88**, 064312 (2013)) have evaluated the non-closure *vs* closure approximation within 10%

Shell model calculations of $M^{0\nu}$

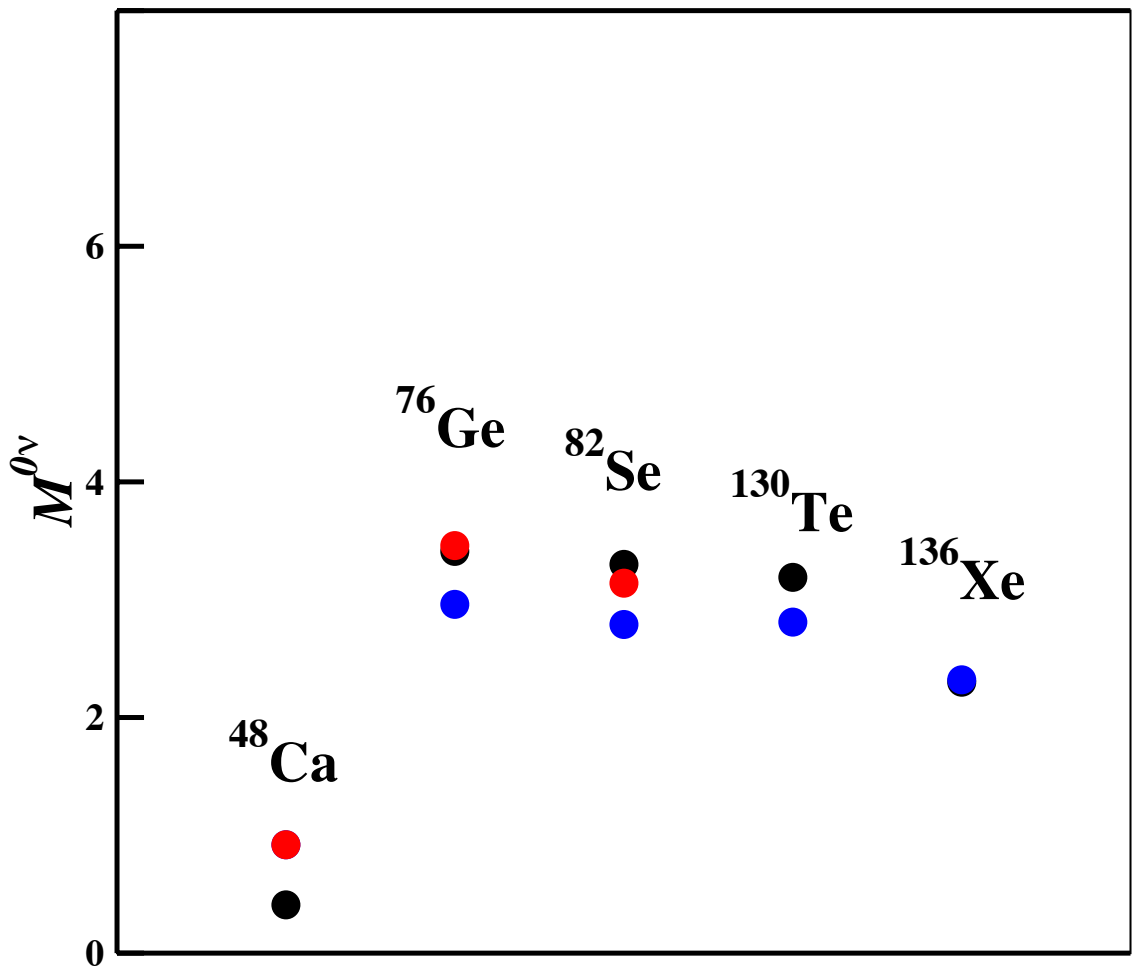

- Blue dots: Madrid-Strasbourg group, bare $0\nu\beta\beta$ operator
- Red dots: Horoi *et al.*, bare $0\nu\beta\beta$ operator
- Black dots: RSM, bare $0\nu\beta\beta$ operator

$0\nu\beta\beta$ decay: short-range correlations

The issue of the SRC for the calculation of $M^{0\nu}$ is framed within the approach of the renormalization of the NN potential

$V_{\mathrm{low-k}}$: the configurations of $V_{NN}(k,k')$ are restricted to those with $k, k' < k_{\mathrm{cutoff}} = \Lambda$

The $V_{\mathrm{low-k}}$ is obtained *via* a unitary transformation Ω

$$\mathcal{H}_{\mathrm{low-k}} = T + V_{\mathrm{low-k}}(k,k') = \Omega^{-1} H_{NN}(k,k')\Omega = T + \Omega^{-1} V_{NN}(k,k')\Omega$$

Consistently, we transform the $0\nu\beta\beta$ operator by way of the same similarity transformation Ω

$$O_{\mathrm{low-k}} = \Omega^{-1} O(k,k')\Omega$$

The SRC affects less than 5%.

For ^{76}Ge: $M^{0\nu}_{\mathrm{bare}} = 3.41 \rightarrow M^{0\nu}_{\mathrm{low-k}} = 3.29$

Perturbative properties of the $0\nu\nu$ effective operator

Convergence with respect the number of intermediate states

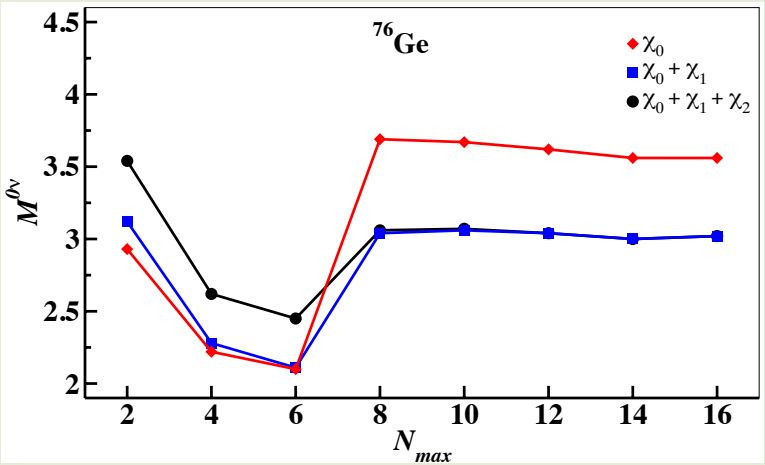

Order-by-order convergence

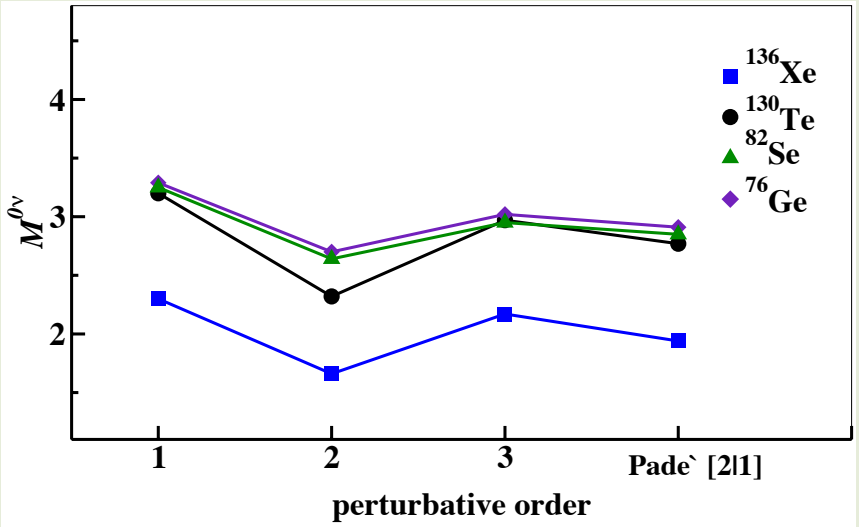

The perturbative behavior is not satisfactory as for the single-β decay operator:
third-order contribution is rather large compared to the second order one

The blocking effect

Blocking (Pauli) effect: as for the one-body operators, the filling of the model-space orbitals by the valence nucleons affects the effective $0\nu\beta\beta$ operator:

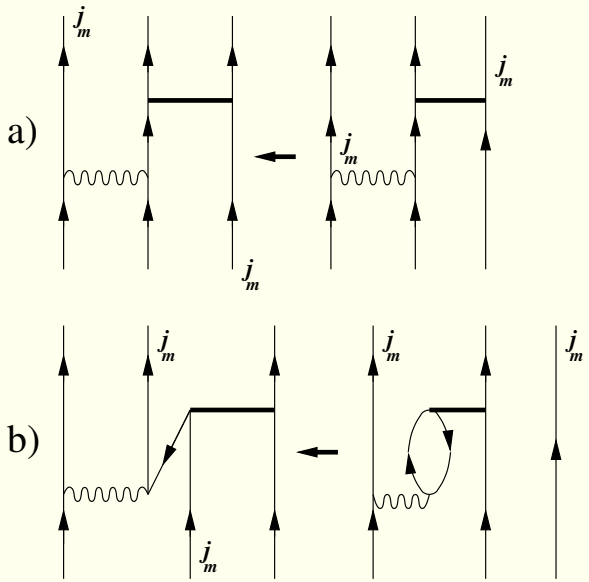

Present shell model codes cannot manage the contributions of these three-body correlations diagrams to the effective $0\nu\beta\beta$-decay operator

The blocking effect

Many-body correlations are then taken into account by calculating three-body correlations diagrams and summing over one of the incoming/outcoming nucleons

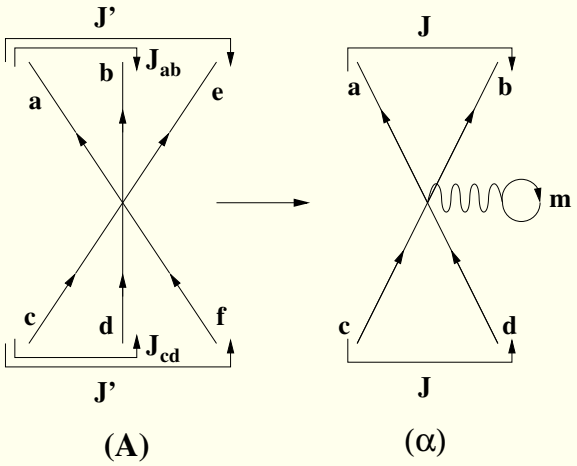

We obtain a density-dependent two-body $0\nu\beta\beta$ effective operator

$$\langle (j_a j_b)_J | O^\alpha | (j_c j_d)_J \rangle = \sum_{m,J'} \rho_m \frac{\hat{J'}^2}{\hat{J}^2} \langle [(j_a j_b)_J, j_m]_{J'} \, | O^A | \, [(j_c j_d)_J, j_m]_{J'} \rangle$$

The blocking effect

Gamow-Teller two-body matrix elements

Decay	$j_a j_b j_c j_d; J = 0^+$	ladder	3b (a)	3p-1h	3b (b)
$^{48}\mathrm{Ca} \rightarrow ^{48}\mathrm{Ti}$					
	$0f_{7/2}0f_{7/2}0f_{7/2}0f_{7/2}$	-0.334	0.004	0.260	-0.017
$^{76}\mathrm{Ge} \rightarrow ^{76}\mathrm{Se}$					
	$0g_{9/2}0g_{9/2}0f_{5/2}0f_{5/2}$	0.154	-0.241	-1.078	0.234
	$0g_{9/2}0g_{9/2}1p_{3/2}1p_{3/2}$	0.185	-0.246	-0.214	0.048
$^{82}\mathrm{Se} \rightarrow ^{82}\mathrm{Kr}$					
	$0g_{9/2}0g_{9/2}0f_{5/2}0f_{5/2}$	0.157	-0.337	-1.096	0.335
	$0g_{9/2}0g_{9/2}1p_{3/2}1p_{3/2}$	0.189	-0.263	-0.219	0.058
$^{130}\mathrm{Te} \rightarrow ^{130}\mathrm{Xe}$					
	$0h_{11/2}0h_{11/2}0g_{7/2}0g_{7/2}$	0.171	-0.202	-0.948	0.297
$^{136}\mathrm{Xe} \rightarrow ^{136}\mathrm{Ba}$					
	$0h_{11/2}0h_{11/2}0g_{7/2}0g_{7/2}$	0.178	-0.264	-0.997	0.381

As we expect:

- 3-body (a) diagram reduces the contribution of the 2-body ladder diagram
- 3-body (b) diagram reduces the contribution of the 2-body 3p-1h (core polarization) diagram

The calculation of $M^{0\nu}$: results

Decay	$M^{0\nu}_{\rm bare}$	$M^{0\nu}_{\rm src}$	$M^{0\nu}_{\rm eff}$	$M^{0\nu}_{\rm eff+3b}$	
$^{48}\mathrm{Ca} \rightarrow ^{48}\mathrm{Ti}$	0.53	0.53	0.30	0.30	-40%
$^{76}\mathrm{Ge} \rightarrow ^{76}\mathrm{Se}$	3.41	3.29	3.02	2.66	-20%
$^{82}\mathrm{Se} \rightarrow ^{82}\mathrm{Kr}$	3.30	3.25	2.95	2.73	-20%
$^{130}\mathrm{Te} \rightarrow ^{130}\mathrm{Xe}$	3.19	3.14	2.97	3.19	0%
$^{136}\mathrm{Xe} \rightarrow ^{136}\mathrm{Ba}$	2.30	2.30	2.17	2.34	$+2\%$

The role of the blocking effect is relevant and, as it should be expected, the final results depend on the number of valence nucleons involved in the shell-model calculation.

Without the blocking effect there is a suppression about 10% with respect the results with the bare operator

Outlook

- Calculation of the effective $0\nu\beta\beta$ beyond the closure approximation
- Derivation of H_{eff} from chiral two- and three-body potentials
- Evaluation of the effects of chiral two-body currents (for both $2\nu\beta\beta$ and $0\nu\beta\beta$ decays)